Hindawi
Journal of Nanomaterials
Volume 2023, Article ID 8767080, 8 pages
https://doi.org/10.1155/2023/8767080

Research Article

Phytochemical-Mediated Synthesis of Nanozinc Oxide Particles and Its Antibacterial, Photocatalytic Degradation of Methylene Blue

Siva Sankar Sana,[1] Ramakrishna Vadde,[2] Sai Kumar Arla,[1] Vijaya Kumar Naidu Boya,[1] Palanivel Velmurugan,[3] Arunachalam Chinnathambi,[4] Sulaiman Ali Alharbi,[4] Subpiramaniyam Sivakumar,[5] and Vijay Singh Kunwar[6]

[1]*Department of Materials Science and Nanotechnology, Yogi Vemana University, Kadapa, 516005 Andhra Pradesh, India*
[2]*Department of Biotechnology and Bioinformatics, Yogi Vemana University, Kadapa, 516005 Andhra Pradesh, India*
[3]*Centre for Materials Engineering and Regenerative Medicine, Bharath Institute of Higher Education and Research, Selaiyur, Chennai, 600073 Tamil Nadu, India*
[4]*Department of Botany and Microbiology, College of Science, King Saud University, PO Box 2455, Riyadh 11451, Saudi Arabia*
[5]*Department of Bioenvironmental Energy, College of Natural Resource and Life Science, Pusan National University, Miryang 50463, Republic of Korea*
[6]*Department of Biotechnology, Himalayan Whitehouse International College, Kathmandu 44600, Nepal*

Correspondence should be addressed to Vijaya Kumar Naidu Boya; drvijayboya@gmail.com
and Vijay Singh Kunwar; vijayskunwar@whitehousecmt.edu.np

Received 29 May 2022; Accepted 9 September 2022; Published 19 April 2023

Academic Editor: Aziz Eftekhari

Using aqueous leaf extract of *Givotia moluccana*, we offer a bioreduction technique for phytochemical-mediated production of nanozinc oxide (N-ZnOPs) particles. Phytochemicals such as polyphenols, flavonoids, and proteins were discovered in the water extract. UV–visible spectroscopy (UV-Vis), Fourier transform infrared spectroscopy (FT-IR), X-ray diffraction (X-RD), and transmission electron microscopy (TEM) are as follows. The UV–visible spectra of synthesized N-ZnOPs revealed absorption peaks at 370 nm. The crystalline nature of ZnO was confirmed by X-RD pattern analyses. Furthermore, TEM pictures demonstrate the creation of hexagonal-shaped N-ZnOPs with diameters ranging from 20 to 50 nm, which is also confirmed by the particle size analyzer, DLS. The synthesized N-ZnOPs displayed antibacterial action as well as photocatalytic destruction of methylene blue (MB) dye, in contrast to gram +ve and gram–ve bacteria. Using the biosynthesis pathway, the current study presents a simple, ecofriendly, and uncomplicated route for the creation of N-ZnOPs. N-ZnOPs are utilized in rubber, paint, coating, and cosmetics. N-ZnOPs are attractive in biological applications due to their biocompatibility, cost, and low toxicity.

1. Introduction

A new method of making nanoparticles from plants has gained popularity among scientists. At ambient temperature, ZnO exhibits a wide bandgap (3.37 eV) semiconductor with deep violet/borderline ultraviolet (UV) absorption [1, 2]. As a nanoscale semiconductor, zinc oxide is used in optical, electronic, optoelectronic, biomedical, rubber, and antibacterial applications and food packaging [3]. Various physical and chemical methods have been used to produce metallic nanoparticles on a large scale, including precipitation, microwave-assisted combustion, sol-gel, and pulsed laser deposition [4]. In choosing green synthesis, the cost of processing, which ultimately harms the ecosystem, is a fundamental consideration. Recently, it has been discovered that seeds, leaves, barks, plant biomass, and microorganisms have the potential to synthesize

nanoparticles in an environmentally friendly and cost-effective manner [5]. In a single process, the phytochemicals that are present in plant parts serve the twin roles of effective reducing agents to reduce the metal zinc and stabilizers to give a durable coating on the zinc nanoparticles [6, 7]. Metal nanoparticles are manufactured from phytochemicals found in aqueous leaf extracts, including tannins, saponins, alkaloids, terpenoids, and flavonoids [8]. Due to their proapoptotic and antiproliferative qualities, natural sources are gaining popularity as anticancer immunity boosters, which are safe, nontoxic, and freely available. Traditional remedies include *Catharanthus roseus* and *Morinda citrifolia*. These two plants have biophores that are anticancer, antifungal, antiviral, antimicrobial, and anti-inflammatory [9]. Zinc is the essential trace element in the human system, second only to iron, in terms of biocompatibility. [10] found that metal oxide NPs can be changed by taking away different atoms and changing their chemical surface properties. This improves their optical, mechanical, and electrical properties.

Zinc oxide nanoparticles (N-ZnOPs) were employed in various applications, including cosmetics, biomedicine, and semiconductors. They may be used as light detectors and semiconductors due to their excitation energy, bandgap, and UV absorption ability. Furthermore, N-ZnOPs have good antibacterial and antifungal properties [11]. Various businesses create more than 528 tonnes of N-ZnOPs every year, according to statistics data, and have documented the phytotoxicity of N-ZnOPs and their nature towards plant structure, physiology, and other aspects [12]. Plant growth inhibition is invariably linked to the form and size of the NPs [13]. The Euphorbiaceae family includes *Givotia moluccana* (*G. moluccana*) and the white catamaran tree [14]. The leaves and roots of this plant have medicinal properties. Carbohydrates, flavonoids, alkaloids, proteins, phenolic compounds, and amino acids are among the phytochemicals found in the leaf extract [15]. Due to drug usage, drug resistance has spread worldwide, and the environmental effects of dye are now a worldwide concern [16]. Alternative methods and medications are required to overcome these limitations in cancer treatment. Researchers are now experimenting with ecofriendly-based nanoparticles as an alternative to inhibiting malignant cell proliferation [17]. Antibacterial activity, photocatalytic dye degradation, and practicality of usage as an antibacterial agent were all investigated for the produced N-ZnOPs.

Based on the previous reviews, this effort attempted to design N-ZnOPs through green synthesis employing *G. moluccana* to target pathogenic bacteria and to clean environment. The novelty of the N-ZnOPs show promise in biomedicine, especially in anticancer and antibacterial fields, due to their capacity to stimulate excess reactive oxygen species (ROS) generation, release zinc ions, and induce cell death.

2. Materials and Methods

2.1. Plant Materials. Yogi Vemana University in Kadapa, India, provided fresh *G. moluccana* plants. HiMedia Laboratories in India provided Muller Hinton agar (MHA) and zinc sulfate (ZnSO4).

2.2. Preparation of Aqueous Extract and N-ZnOP Fabrication. *G. moluccana* fresh leaves were collected, washed in running tap water followed by Milli-Q water, and then shade-dried. The ground 10 g of powder was mixed in 100 mL of Milli-Q water in a 250 mL Erlenmeyer flask and boiled for 30 min at 80°C. After this, the extract was filtered using Whatman No. 1 filter paper, and the filtrate was used for a subsequent experiment. To prepare N-ZnOPs, a known amount of zinc nitrate salt was dissolved in 20 mL of extract and heated in the reaction mixture till the yellow precipitate appeared. The reaction mixture was kept in a muffle furnace at 400°C for 3 h for calcination. Finally, N-ZnOPs were obtained in white color powder that was stored in labeled containers for further use.

2.3. Physical Characterization. A UV–Vis spectrophotometer was used to validate the dried N-ZnOP identity. Using a Fourier transform infrared (FT-IR) spectrophotometer and the KBr pellet technique in the spectrum region of 4000–500 cm^{-1}, the functional groups and phytochemicals involved in the reactivity of NPs were identified. X-ray diffractometer was used to examine the XRD pattern of green-produced N-ZnOPs. The precise form, size, and dispersive character of the N-ZnOPs were also recorded using TEM. Energy dispersive X-ray spectrometer was used to study the topographical structure and atomic composition (EDX). EDX was used to examine the composition purity and elemental mapping of N-ZnOPs.

2.4. Antimicrobial Activity. The antibacterial activity of N-ZnOPs toward the selected pathogens *Escherichia coli* (*E. coli*) and *Staphylococcus aureus* (*S. aureus*) was studied by using the good diffusion method. The set of two dilutions ((a) 50 and (b) 75 μg/mL) of N-ZnOP colloidal solution in the disc was prepared and used in this study. Sterile Muller Hinton agar plates were seeded with respective bacterial strains at 10^8 CFU. At three corners of the Petri plates, two different concentrations of the N-ZnOPs were placed over the lawn of bacterial culture along with positive control and streptomycin ((c) 30 μg/mL. Plates were incubated at 37°C overnight. The zone of inhibition (ZOI) (mm) was measured after 24 h, and the results were expressed as ZOI in mm in the table. This experiment was conducted in triplicate.

2.5. Photocatalytic Activity. The degradation of methylene blue (MB), a known amount of synthesized catalyst, was added to MB (10 ppm) solution and stirred at 200 rpm for 30 min in the dark to get adsorption in the semiconductor surface by the MB, during the middle of the May month. The solution was irradiated for regular intervals of time under sunlight. In each stage, the collected sample aliquot was centrifuged at 5000 rpm to separate catalyst particles and analyzed at 664 nm by UV–visible spectrophotometer.

$$\%\text{Degradation} = \frac{((C_0) - (C_t))}{((C0))} \text{X}100, \quad (1)$$

where C_0 and C_t will be the initial and final amount of MB solution, respectively.

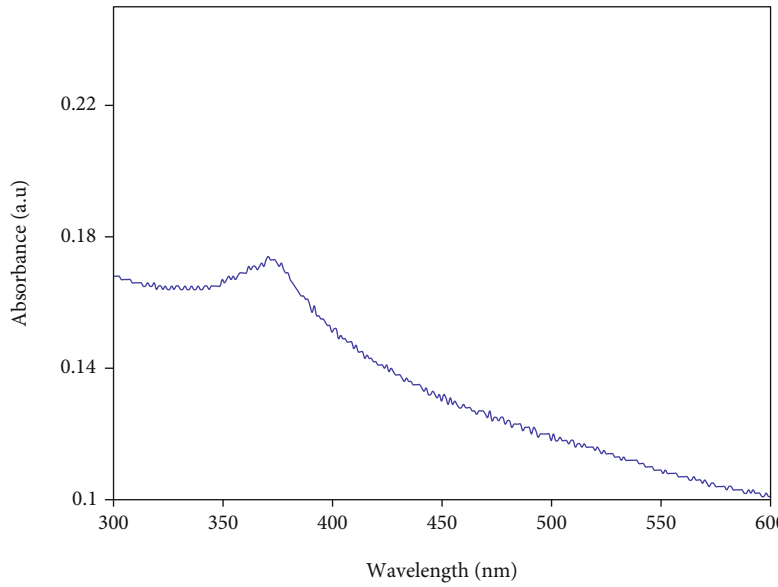

Figure 1: shows the UV-visible spectrum of N-ZnOPs.

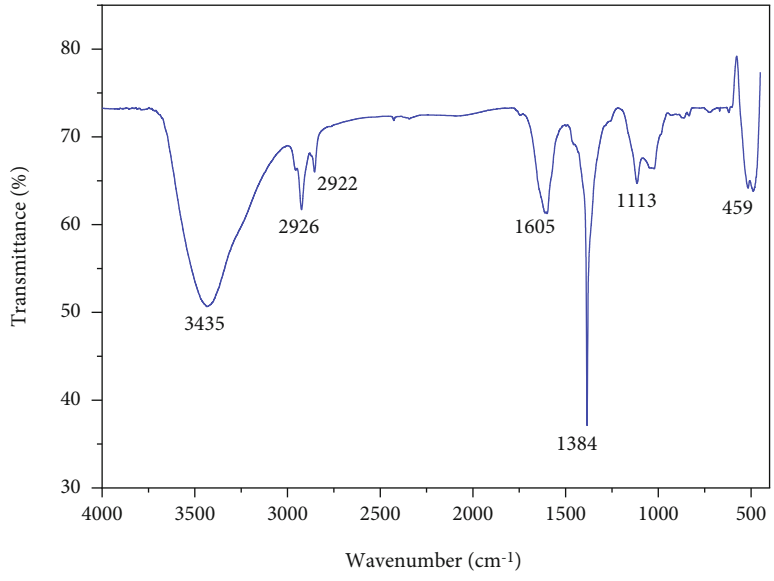

Figure 2: FT-IR spectrum of green-produced N-ZnOPs.

3. Results and Discussion

The aqueous extract of *G. moluccana* contains 40.4 ± 1.6 GAE/gm, 8.8 ± 0.05 RE/gm and 30.53 ± 0.3 mg/gm of polyphenols, flavonoids, and proteins, respectively. The results of the analysis put forward the information that the extract of aqueous leaf is an excellent starting material of bioactive phytochemicals that can effectively involve in reducing and stabilization of the particles during the fabrication [18]. The absorption peak was observed for N-ZnOPs at a wavelength of 370 nm due to the surface plasmon resonance of nanoparticles (Figure 1). The results are well to an earlier report on the green synthesis of N-ZnOPs by [19].

The peaks at 3435 and 2922 cm^{-1} are due to hydroxyl (-OH) as well as aldehydes C–H, respectively [20]. The peak at 2926 and 1605 cm^{-1} corresponds to symmetric stretching of carboxyl groups stretching of C–H in alkenes and stretching of carboxyl groups, respectively. A peak at 459 cm^{-1} lowers frequency that matches with particles of Zn-O with vibration bond bending (Figure 2) [21].

The previous reports also suggest that secondary metabolites like polyphenols and flavonoids are responsible for the

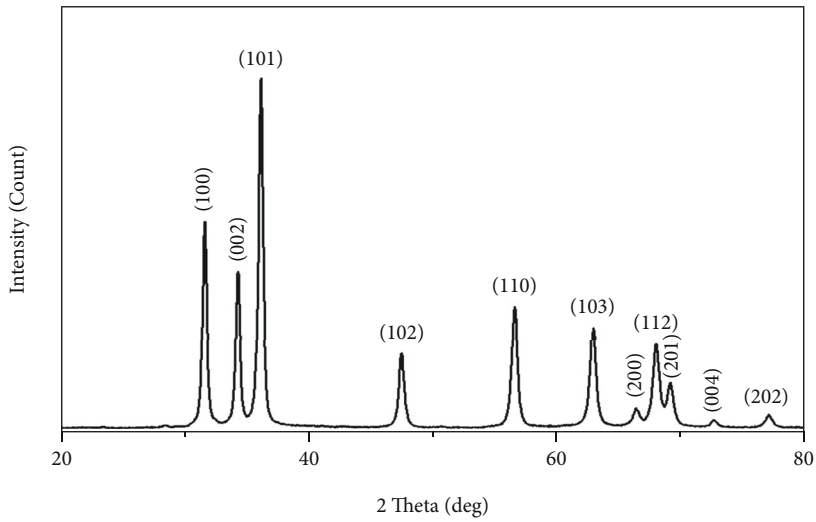

Figure 3: XRD spectrum of green N-ZnOPs produced.

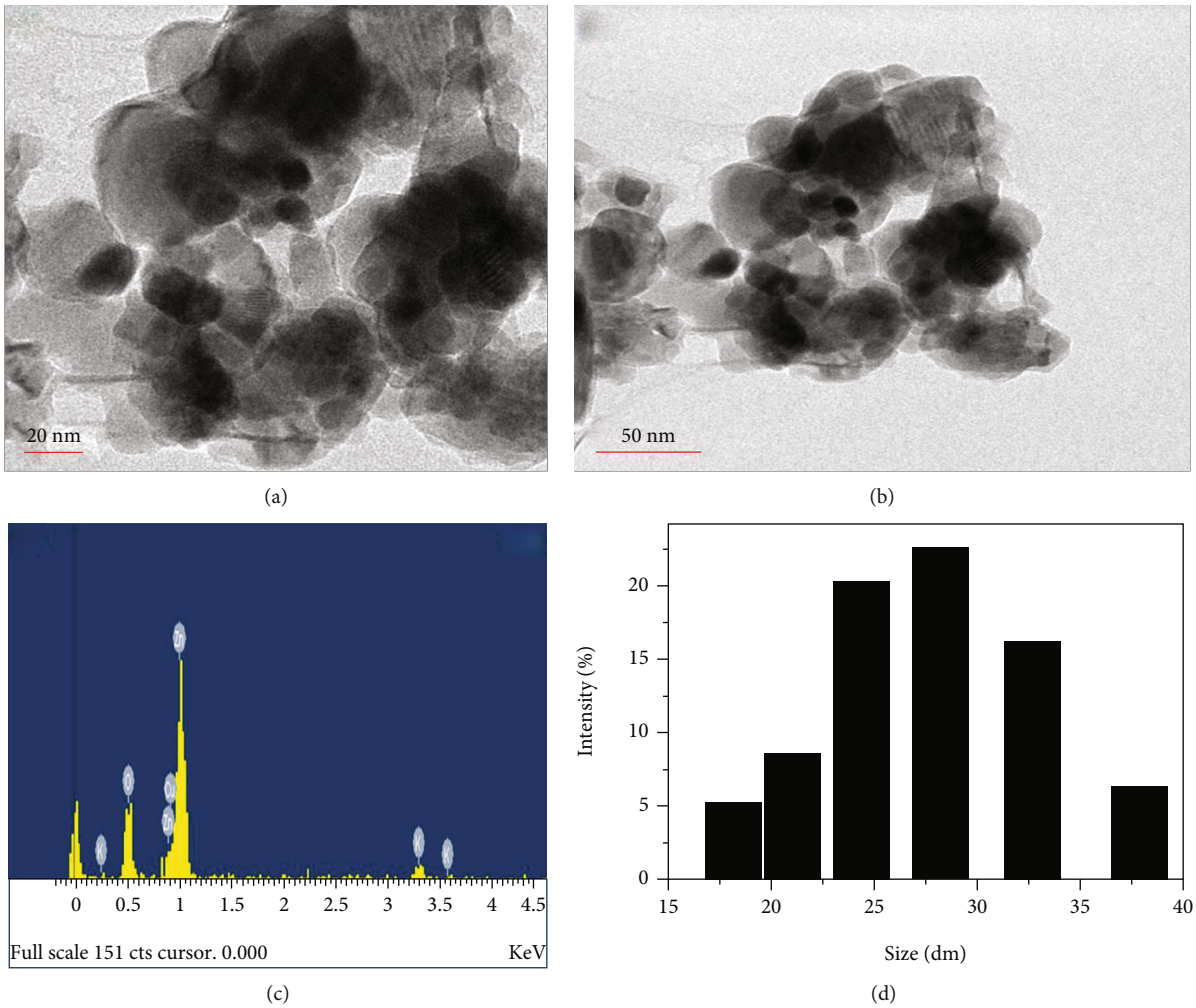

Figure 4: TEM images of green synthesized N-ZnOPs: (a) (20 nm) and (b) (50 nm). EDX pattern of green synthesized N-ZnOPs and particle size histogram.

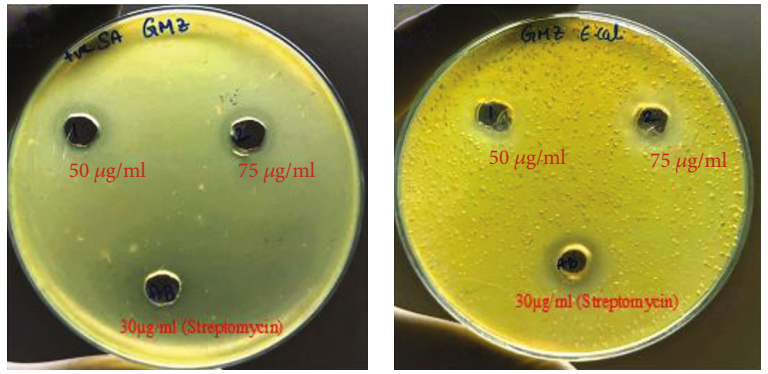

(a) (b)

Figure 5: Images of antibacterial activity of green-produced N-ZnOPs.

Table 1: Antibacterial activity results.

S. no	Microorganism	Zone of inhibition (ZOI) (mm)		
		50 μg/mL	75 μg/mL	Streptomycin 30 μg/mL
1.	*E. coli*	13 ± 1.0	15 ± 0.4	16 ± 1.4
2.	*S. aureus*	16 ± 1.2	18 ± 0.5	21 ± 1.7

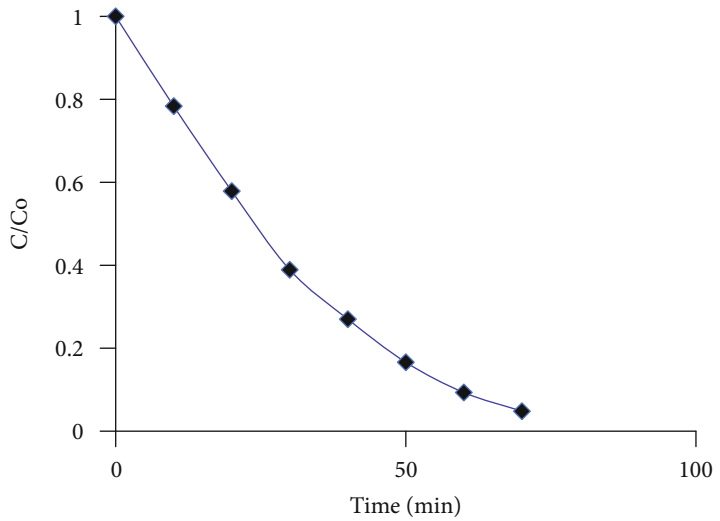

Figure 6: Photocatalytic effectiveness of green-produced N-ZnOPs on methylene blue degradation (MB).

reduction and stabilization and also amino as well as carboxylic groups of proteins which are present in the leaf extract [18, 22].

The diffraction results through XRD of zinc oxide particles are obtained at 2θ values, and peak includes 31.50, 34.19, 36.05, 47.35, 56.34, 62.65, 66.19, 67.76, 68.92, 72.41, and 76.77° that correlates to the (100), (002), (101), (102), (110), (103), (200), (112), (201), (004), and (202) planes, respectively [23]. From the above information on diffraction, the hexagonal patterns indexed to quartzite structured ZnO are identified, as shown in Figure 3. Image captured by TEM analysis of green N-ZnOPs produced, EDX spectrum, and particle size is represented in Figures 4(a)–4(d).

TEM microscopy was used to examine the morphology of the produced N-ZnOPs. The produced N-ZnOPs were rod-shaped with aggregation and ranged in size from 40 to 50 nm, according to TEM images (Figures 4(a) and 4(b)). The aggregation of N-ZnOPs was likely caused by the presence of *G. moluccana* hydrous extract all around the N-ZnOPs, gluing them together. The elemental mapping study

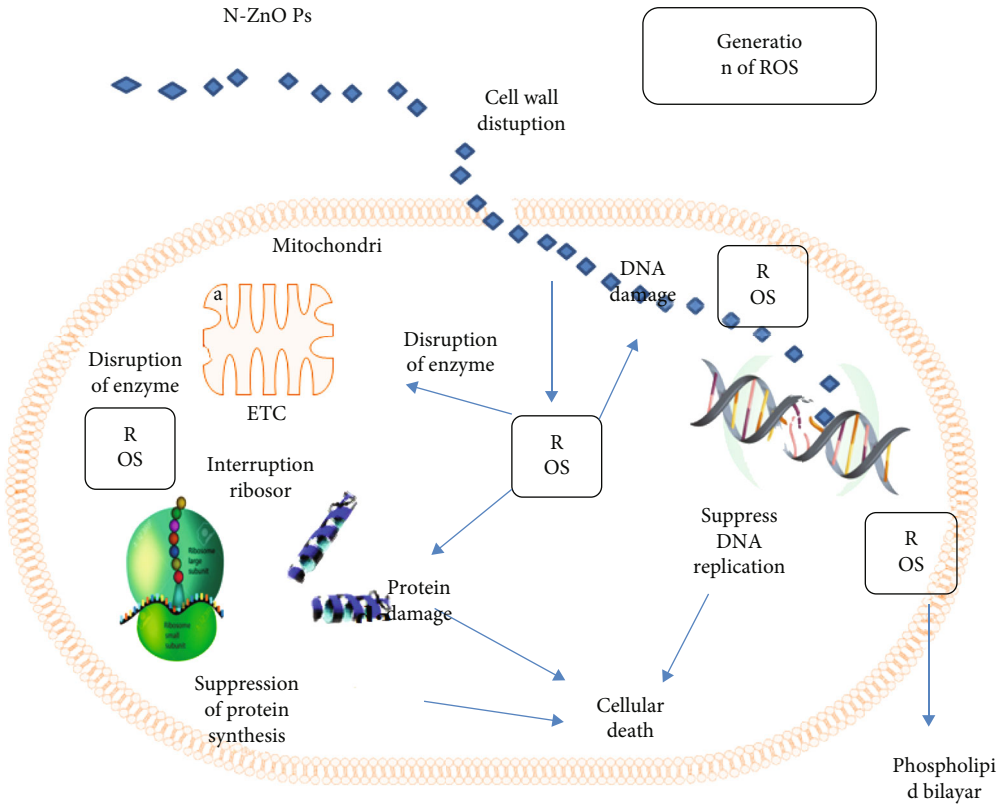

Figure 7: Schematic diagram of MB degradation by green generated ZnO NPs.

looked at how Zn and other elements were distributed in the N-ZnOPs that had been created. The elemental mapping of the N-ZnOPs produced with *G. moluccana* aqueous extract indicated that the generated NPs comprised zinc (66.25%) as the main element, with oxygen (33.75%) and other elements present in the NPs (Figure 4(c)). Figure 4(d) shows the size distribution of the N-ZnOPs calculated from more than 250 particles.

As biosynthesized N-ZnOPs were tested with gram-negative, gram-positive stains revealed the effective suppressive activity of these nanoparticles, and the results were presented in Figure 5 and Table 1. The antibacterial effect of nanoparticles depends on their size: the smaller the size, the higher the activity. Records show that particle size is the main factor affecting the sensitivity of bacteria towards nanomaterials. Electrostatic interactions between ZnO and cell walls and the high surface area to volume ratio result in destroying bacterial cell integrity, thereby enhancing its antimicrobial activity. The nanoparticles interfere with cellular processes and immobilize them by adhesion to the microbial cell surface [24]. N-ZnOPs may also enter into a bacterial cell and aims for making harmful radicals related to the oxygen that break bacterial genetic material and proteins of the cell leading to the inhibition as well as the death of the organism. Also, the interaction of microbial functional groups like thiol protein on the bacterial surface leads to a less permeable rate which finally ends up in lysis [24].

Using aqueous solutions of MB dye and a natural irradiation approach, the photocatalytic property of N-ZnOPs was investigated. At various time intervals during the degradation of MG and MB dyes, varied absorption spectra were observed (Figure 6). The greatest elimination percentage of the produced N-ZnOPs was 80 percent MB. In comparison to earlier published data, the current study found a greater rate of deterioration. Biological synthesis methods are, on average, less harmful than most traditional synthesis processes. As a result, the current manufacturing process and capacity to break down synthetic dyes were more effective than in prior investigations [16, 25, 26]. In contrast to bigger-sized particles, the zone of inhibition produced by the tiniest particle sizes, known as nanoparticles, was discovered to be significantly greater (about 19 millimeters) in size. A bigger surface area-to-volume ratio of samples can be ascribed to the fact that nanoparticles are discovered to be more poisonous than other nanoparticles. This is because larger particle-sized nanoparticles have a smaller surface area relative to their volume. Because of their greater surface area, particles of smaller size are better able to interact with the membranes of bacteria, which contributes to an increase in the effectiveness of these particles as antibacterial agents. It has been demonstrated that the concentration of nanoparticles has an effect on this size dependency of antibacterial activity [27].

In addition, antioxidants stop free radical chain reactions and turn them into harmless compounds. Antioxidants reduce oxidative stress and treat free radical-related illnesses. Their low absorption, inability to cross cell membranes, and disintegration during delivery limit their bioavailability. Antioxidants covalently coupled with nanoparticles, entrapped in nanogel, hollow particles, or encapsulated into nanoparticles of varied

origin give greater stability, gradual and prolonged release, biocompatibility, and targeted administration of antioxidants with superior antioxidant profiles.

A schematic diagram of MB degradation (Figure 7) and UV-visible spectra of decomposed MB are displayed in Figure 6. The amount percentage of debarring and pie chart of degradation are mentioned in Figures 6 and 7. The catalyst activity begins with the generation of an electron-hole (e^-–h^+) pair under sunlight. When the catalyst gets irradiated with sunlight, the electron gets excited and displaces from the valence to the conduction band by making a hole that will react with oxygen as well as hydroxyl and formation radicals of hydroxyl (•OH), radical anions of superoxide ($\cdot O_2^-$), and radicals of hydroperoxyl ($\cdot O_2H$) occur. Among all the reactive species, hydroxyl is more powerful and can attack MB present in the reaction medium at the surface of the catalyst [28]. Most importantly, the optical density at λ_{max} of MB gets reduced with the rate of reaction time which mentions decolonization [29].

4. Conclusion

Green production of ZnO nanoparticles has been achieved by the use of aqueous leaf extract *Givotia moluccana*. The formation of N-ZnOPs was characterized by UV-vis, FT-IR, TEM, and XRD shape and size control of nanoparticles. Analysis of the FT-IR spectrum shows the presence of phenols that helps in the conversion from Zn^{2+} to zinc oxide. TEM micrographs reveal that the particles were almost hexagonal that is varying from about 18 to 38 nm. The formed N-ZnOPs show crystalline and attained a size below 50 nm as evidenced by TEM and XRD. The results showed that the synthesized N-ZnOPs are useful as good antimicrobial and catalyst material.

Data Availability

The data used to support the findings of this study are included in the article. Should further data or information be required, these are available from the corresponding authors upon request.

Conflicts of Interest

The authors declare that there are no conflicts of interest regarding the publication of this paper.

Acknowledgments

The authors are grateful to the DST-TDT-SHRI (DST/TDT/SHRI-06/2021) for providing the financial assistance in this project. We specially express our thanks to the management of Bharth Institute of Higher Education and Research, Chennai, for providing the necessary facilities and support to carry out this work. This project was supported by the Researchers Supporting Project (number RSP-2022/5) of King Saud University, Riyadh, Saudi Arabia.

References

[1] B. Kumar, K. Smita, L. Cumbal, and A. Debut, "Green approach for fabrication and applications of zinc oxide nanoparticles," *Bioinorganic Chemistry and Applications*, vol. 2014, Article ID 523869, 7 pages, 2014.

[2] D. Jain, A. A. Bhojiya, H. Singh et al., "Microbial fabrication of zinc oxide nanoparticles and evaluation of their antimicrobial and photocatalytic properties," *Frontiers in Chemistry*, vol. 8, p. 778, 2020.

[3] S. Raha and M. Ahmaruzzaman, "ZnO nanostructured materials and their potential applications: progress, challenges and perspectives," *Nanoscale Advances*, vol. 4, no. 8, pp. 1868–1925, 2022.

[4] M. Hasanpoor, M. Aliofkhazraei, and H. Delavari, "Microwave-assisted synthesis of zinc oxide nanoparticles," *Procedia Materials Science*, vol. 11, pp. 320–325, 2015.

[5] R. K. Das, V. L. Pachapur, L. Lonappan et al., "Biological synthesis of metallic nanoparticles: plants, animals and microbial aspects," *Nanotechnology for Environmental Engineering*, vol. 2, no. 1, pp. 1–21, 2017.

[6] A. C. Paiva-Santos, A. M. Herdade, C. Guerra et al., "Plant-mediated green synthesis of metal-based nanoparticles for dermopharmaceutical and cosmetic applications," *International Journal of Pharmaceutics*, vol. 597, article 120311, 2021.

[7] A. R. Prasad, L. Williams, J. Garvasis et al., "Applications of phytogenic ZnO nanoparticles: a review on recent advancements," *Journal of Molecular Liquids*, vol. 331, p. 115805, 2021.

[8] V. Jadhav, A. Bhagare, I. H. Ali et al., "Role of Moringa oleifera on green synthesis of metal/metal oxide nanomaterials," *Journal of Nanomaterials*, vol. 2022, Article ID 2147393, 10 pages, 2022.

[9] K. P. Greeshma and R. Thamizselvi, "Experimental and theoretical approach on green synthesized zinc oxide nanoparticles from combined leaf extracts of _Catharanthus roseus_ and _Morinda Citrifolia for_ invitro anti-cancer studies," *Journal of Molecular Liquids*, vol. 351, p. 118636, 2022.

[10] S. Mourdikoudis, R. M. Pallares, and N. T. Thanh, "Characterization techniques for nanoparticles: comparison and complementarity upon studying nanoparticle properties," *Nanoscale*, vol. 10, no. 27, pp. 12871–12934, 2018.

[11] A. Sirelkhatim, S. Mahmud, A. Seeni et al., "Review on zinc oxide nanoparticles: antibacterial activity and toxicity mechanism," *Nano-micro letters*, vol. 7, no. 3, pp. 219–242, 2015.

[12] H. Zafar, A. Ali, J. S. Ali, I. U. Haq, and M. Zia, "Effect of ZnO nanoparticles on Brassica nigra seedlings and stem explants: growth dynamics and antioxidative response," *Frontiers in Plant Science*, vol. 7, p. 535, 2016.

[13] S. Ali, A. Mehmood, and N. Khan, "Uptake, translocation, and consequences of nanomaterials on plant growth and stress adaptation," *Journal of Nanomaterials*, vol. 2021, Article ID 6677616, 17 pages, 2021.

[14] D. Pullaiahgari, R. K. Meena, S. R. Tirupaati, and P. Gudipalli, "Proteomic analysis of differentially abundant proteins in the embryo and endosperm of Givotia moluccana (L) Sreem," *Journal of Forestry Research*, vol. 31, no. 6, pp. 2097–2109, 2020.

[15] J. Senguttuvan, S. Paulsamy, and K. Karthika, "Phytochemical analysis and evaluation of leaf and root parts of the medicinal herb, Hypochaeris radicata L for in vitro antioxidant activities," *Asian Pacific Journal of Tropical Biomedicine*, vol. 4, no. 1, pp. S359–S367, 2014.

[16] B. Lellis, C. Z. Fávaro-Polonio, J. A. Pamphile, and J. C. Polonio, "Effects of textile dyes on health and the environment and bioremediation potential of living organisms," *Biotechnology Research and Innovation*, vol. 3, no. 2, pp. 275–290, 2019.

[17] J. J. Xu, W. C. Zhang, Y. W. Guo, X. Y. Chen, and Y. N. Zhang, "Metal nanoparticles as a promising technology in targeted cancer treatment," *Drug Delivery*, vol. 29, no. 1, pp. 664–678, 2022.

[18] G. K. Weldegebrieal, "Synthesis method, antibacterial and photocatalytic activity of ZnO nanoparticles for azo dyes in wastewater treatment: a review," *Inorganic Chemistry Communications*, vol. 120, article 108140, 2020.

[19] G. Marslin, K. Siram, Q. Maqbool et al., "Secondary metabolites in the green synthesis of metallic nanoparticles," *Materials*, vol. 11, no. 6, p. 940, 2018.

[20] P. C. Nagajyothi, T. V. M. Sreekanth, C. O. Tettey, Y. I. Jun, and S. H. Mook, "Characterization, antibacterial, antioxidant, and cytotoxic activities of ZnO nanoparticles using Coptidis Rhizoma," *Bioorganic & Medicinal Chemistry Letters*, vol. 24, no. 17, pp. 4298–4303, 2014.

[21] M. H. Kahsay, "Synthesis and characterization of ZnO nanoparticles using aqueous extract of Becium grandiflorum for antimicrobial activity and adsorption of methylene blue," *Applied Water Science*, vol. 11, no. 2, pp. 1–12, 2021.

[22] S. S. Sana, D. V. Kumbhakar, A. Pasha et al., "Crotalaria verrucosa leaf extract mediated synthesis of zinc oxide nanoparticles: assessment of antimicrobial and anticancer activity," *Molecules*, vol. 25, no. 21, p. 4896, 2020.

[23] A. M. Awwad, M. W. Amer, N. M. Salem, and A. O. Abdeen, "Green synthesis of zinc oxide nanoparticles (ZnO-NPs) using Ailanthus altissima fruit extracts and antibacterial activity," *Chemistry International*, vol. 6, no. 3, pp. 151–159, 2020.

[24] B. Bonev, J. Hooper, and J. Parisot, "Principles of assessing bacterial susceptibility to antibiotics using the agar diffusion method," *The Journal of Antimicrobial Chemotherapy*, vol. 61, no. 6, pp. 1295–1301, 2008.

[25] A. Baran, M. Fırat Baran, C. Keskin et al., "Investigation of Antimicrobial and Cytotoxic Properties and Specification of Silver Nanoparticles (AgNPs) Derived from Cicer Arietinum L Green Leaf Extract," *Frontiers in Bioengineering and Biotechnology*, vol. 10, p. 263, 2022.

[26] A. Hasanzadeh, B. Gholipour, S. Rostamnia et al., "Biosynthesis of AgNPs onto the urea-based periodic mesoporous organosilica (Ag_xNPs/Ur-PMO) for antibacterial and cell viability assay," *Journal of Colloid and Interface Science*, vol. 585, pp. 676–683, 2021.

[27] Q. U. A. Naqvi, A. Kanwal, S. Qaseem et al., "Size-dependent inhibition of bacterial growth by chemically engineered spherical ZnO nanoparticles," *Journal of Biological Physics*, vol. 45, no. 2, pp. 147–159, 2019.

[28] G. Yu, Y. Wang, H. Cao, H. Zhao, and Y. Xie, "Reactive oxygen species and catalytic active sites in heterogeneous catalytic ozonation for water purification," *Environmental Science & Technology*, vol. 54, no. 10, pp. 5931–5946, 2020.

[29] C. B. Ong, L. Y. Ng, and A. W. Mohammad, "A review of ZnO nanoparticles as solar photocatalysts: synthesis, mechanisms and applications," *Renewable and Sustainable Energy Reviews*, vol. 81, pp. 536–551, 2018.